DEVELOPMENTAL BIOLOGY

Synthetic presentation of noncanonical Wnt5a motif promotes mechanosensing-dependent differentiation of stem cells and regeneration

Rui Li[1], Sien Lin[2], Meiling Zhu[2], Yingrui Deng[1], Xiaoyu Chen[1], Kongchang Wei[3], Jianbin Xu[4], Gang Li[2], Liming Bian[1,5,6,7]*

Noncanonical Wnt signaling in stem cells is essential to numerous developmental events. However, no prior studies have capitalized on the osteoinductive potential of noncanonical Wnt ligands to functionalize biomaterials in enhancing the osteogenesis and associated skeleton formation. Here, we investigated the efficacy of the functionalization of biomaterials with a synthetic Wnt5a mimetic ligand (Foxy5 peptide) to promote the mechanosensing and osteogenesis of human mesenchymal stem cells by activating noncanonical Wnt signaling. Our findings showed that the immobilized Wnt5a mimetic ligand activated noncanonical Wnt signaling via the up-regulation of Disheveled 2 and downstream RhoA-ROCK signaling, leading to enhanced intracellular calcium level, F-actin stability, actomyosin contractility, and cell adhesion structure development. This enhanced mechanotransduction in stem cells promoted the in vitro osteogenic lineage commitment and the in vivo healing of rat calvarial defects. Our work provides valuable guidance for the developmentally inspired design of biomaterials for a wide array of therapeutic applications.

INTRODUCTION

Human mesenchymal stem cells (hMSCs) have become increasingly popular as a cell source for repairing bone and other musculoskeletal tissues due to their availability, accessibility, and multipotency (*1*). The lineage commitment of hMSCs has been shown to be regulated by various signals, including mechanical stimuli, soluble factors, and cell–extracellular matrix (ECM) interactions, in their natural niche microenvironment (*2*). Meanwhile, the delayed reunion of fractured bone remains a major clinical complication of surgery despite advances in operative techniques. The direct injection of stem cells into bone defects generally leads to limited stem cell grafting and differentiation due to the lack of necessary biochemical cues in the defect sites (*3*). Developing osteoinductive biomaterial scaffolds by incorporating developmentally relevant signaling cues to support and guide the differentiation of implanted stem cells in situ will enhance the clinical outcomes of stem cell therapies (*4*). For instance, scaffolds have been decorated with a wide range of bioactive motifs, including growth factors, bioactive peptides, and small molecules, to boost their osteoinductivity (*5*, *6*). In recent years, biomimetic/bioactive peptides have become increasingly popular as inductive motifs for the biofunctionalization of biomaterials due to their major advantages, including their ease of immobilization onto various biomaterials via bioconjugation, better stability than proteins, and low cost (*7*). We previously demonstrated that the decoration of a hydrogel scaffold with an N-cadherin mimetic peptide promoted the chondrogenesis or the osteogenesis of hMSCs by emulating the enhanced intercellular interactions (*8*, *9*). Therefore, there is an acute demand for previously unidentified osteoinductive ligands, which can potentially be identified by examining developmentally relevant proteinaceous cues (*10*).

Wnt signaling pathways have been reported to be essential to many developmental events, especially osteogenesis and bone formation (*11*, *12*). The canonical Wnt signaling pathways generally involve the preservation and nuclear translocation of β-catenin, which further triggers the activation of downstream genes to initiate osteogenic differentiation (*13*). On the other hand, the β-catenin–independent noncanonical Wnt signaling cascade is activated by noncanonical Wnt ligands, such as Wnt5a (*14*). Wnt5a activation has been reported to contribute to the regeneration of multiple tissues, including the articular cartilage, the colonic crypt, and the liver, via paracrine or autocrine regulation (*15*–*17*). During in vitro osteogenesis, embryonic stem cells express Wnt5a early on, rather than canonical Wnt3a, and cells expressing Wnt5a or treated with exogenous Wnt5a show a substantially enhanced osteogenic yield (*18*). In trabecular bone and bone marrow, Wnt5a is mainly expressed and secreted by osteoblastic niche cells, including precursor cells, osteoblasts, osteoclasts, and osteocytes (*19*). Wnt5a has been reported to preserve the proliferation and differentiation potential of stem cells in bone marrow and induce osteoblast maturation (*20*). Wnt5a signaling is a substantial constituent of bone morphogenetic protein 2–mediated osteoblastogenesis (*21*). Collectively, these findings indicate that Wnt5a is an essential cue for the development of bones.

Wnt5a signaling is mediated through the Disheveled (Dvl) segment polarity protein–dependent mechanism, which activates the small guanosine triphosphatase (GTPase) RhoA and its effector ROCKs (Rho-associated protein kinases) (*22*). RhoA-ROCK signaling plays a major regulatory role in the mechanotransduction signaling of cells by promoting focal adhesion formation (*16*), stress fiber assembly (*23*), and actomyosin contractility, and all these cellular events have been shown to enhance the osteogenesis of mesenchymal stem cells (MSCs). However, to the best of our knowledge, no prior studies have capitalized on the osteoinductive potential of noncanonical Wnt ligands to functionalize biomaterials or investigated the efficacy

[1]Department of Biomedical Engineering, The Chinese University of Hong Kong, Sha Tin, New Territories 999077, Hong Kong, P. R. China. [2]Department of Orthopaedics and Traumatology, Faculty of Medicine, The Chinese University of Hong Kong, Sha Tin, New Territories 999077, Hong Kong, P. R. China. [3]Empa, Swiss Federal Laboratories for Materials Science and Technology, Laboratory for Biomimetic Membranes and Textiles, Lerchenfeldstrasse 5, CH-9014 St. Gallen, Switzerland. [4]Biomedical Research Center, Sir Run Run Shaw Hospital, School of Medicine, Zhejiang University, Hangzhou, Zhejiang 310016, P. R. China. [5]Shenzhen Research Institute, The Chinese University of Hong Kong, Sha Tin, New Territories 999077, Hong Kong, P. R. China. [6]China Orthopedic Regenerative Medicine Group (CORMed), Hangzhou, P. R. China. [7]Center of Novel Biomaterials, The Chinese University of Hong Kong, Sha Tin, New Territories, 999077 Hong Kong, P.R. China.
*Corresponding author. Email: lbian@cuhk.edu.hk

of such a developmental biology–inspired strategy to enhance the osteogenesis of MSCs and associated bone formation.

Recently, a Wnt5a mimetic hexapeptide, Foxy5 (formyl-Met-Asp-Gly-Cys-Glu-Leu), was shown to trigger cytosolic calcium signaling by activating β-catenin–independent noncanonical Wnt signaling (*24*), and Foxy5 has recently been tested in a phase 1 clinical trial for treating cancer (www.clinicalTrials.gov; NCT02020291) (*25*). Here, we hypothesized that the functionalization of biomaterials with Foxy5 peptide can promote the mechanosensing and osteogenesis of hMSCs by activating noncanonical Wnt signaling (Fig. 1A). Our findings showed that this synthetic presentation of Wnt5a mimetic ligand activated noncanonical Wnt signaling, elevated the intracellular calcium, and promoted the mechanotransduction and osteogenesis of hMSCs, resulting in the enhanced bone regeneration in vivo. These findings emphasize the significance of the biofunctionalization of biomaterial scaffolds with developmentally guiding cues to enhance in situ tissue regeneration via grafted stem cells (*26*, *27*).

RESULTS AND DISCUSSIONS

Fabrication of hydrogels presenting the noncanonical Wnt5a cue

To determine the effect of the Wnt5a mimetic peptide (Foxy5) on cellular behaviors, we grafted methacrylated hyaluronic acid (MeHA) with Foxy5 peptide (MDGECL, 1 mM) and arginylglycylaspartic acid (RGD) peptide (GCGYGRGDSPG, 1 mM) via Michael addition between the cysteine thiols of the peptide and the methacrylate groups of the MeHA (Fig. 1A and fig. S1). The peptide-functionalized MeHA (degree of methacryloyl substitution or methacrylation degree = 100 or 30%) (fig. S1) was then cross-linked to fabricate a three-dimensional (3D) porous hydrogel scaffold or a 2D hydrogel substrate for subsequent experiments (Foxy5 + RGD) (Fig. 1, B to D). Control hydrogels were fabricated with either RGD peptide alone (RGD) or the combination of scramble-sequenced Foxy5 peptide and RGD (GEMDCL, 1 mM, Scram + RGD). The RGD peptide was included in all groups to promote cell adhesion. The average Young moduli of the hydrogels from the RGD, Foxy5 + RGD, and Scram + RGD groups were determined to be 11.26, 10.82, and 10.96 kPa, respectively, indicating similar hydrogel stiffness in all groups (Fig. 1E). The storage moduli and loss moduli acquired from the frequency sweep analysis were not significantly different among the RGD, Foxy5 + RGD, and Scram + RGD groups (fig. S2A). Similarly, the surface roughness and the stiffness of 2D ultraviolet (UV)–cross-linked hydrogels are not significantly different (fig. S2B). Our previous experience shows that the photocrosslinked MeHA hydrogels are typically stiffer than the dithiothreitol (DTT)–cross-linked MeHA hydrogels given the same macromer content and methacrylation degree. This can be due to the semirigid nature of hyaluronic acid (HA) backbone, which may hinder the efficient crosslinking of HA-grafted methacryloyl groups by bifunctional crosslinkers (e.g., DTT). Therefore, by using the MeHA with the lower (30%) methacrylation degree to fabricate 2D hydrogels, the average Young moduli of the photocrosslinked hydrogels with 667 s of UV radiation were not significantly different from those of the DTT–cross-linked MeHA hydrogels (100% methacrylation degree) (fig. S2, C and D). We believe that the results acquired from the 2D hydrogel substrates are representative and comparable with the data obtained from the 3D macroporous hydrogels. The 3D porous hydrogels used in this work have large pore sizes of around a few hundred micrometers, which are significantly larger than that of cells. The cells seeded in these 3D hydrogels are essentially still residing on top of the curved surfaces of the pores and are interacting with a more 2D-like rather than 3D microenvironment, and this is similar to the lining of osteoblasts on the surface of porous trabecular bone.

To evaluate the cytocompatibility of the peptide-functionalized hydrogels, we seeded hMSCs into the porous hydrogel constructs and allowed them to adhere for 4 hours, followed by further culture in basal growth media for another 7 days. Live/dead staining after 7 days of culture revealed that the majority of the seeded stem cells were viable and uniformly adhered to the RGD, Foxy5 + RGD, and Scram + RGD porous hydrogels (Fig. 1F). The alamarBlue assay showed that the seeded cells in all groups maintained consistent and robust metabolic activity in the porous hydrogel scaffolds for 7 days (Fig. 1G). These results indicate that the conjugated bioactive Foxy5 peptide was noncytotoxic, consistent with previous reports (*24*).

Foxy5 peptide functionalization enhances the mechanotransduction of hMSCs in 2D and 3D MeHA hydrogels

To further investigate the molecular events mediated by the noncanonical Wnt5a mimetic Foxy5 peptide, we used immunofluorescence staining to examine the expression levels of integrin α_V, integrin β_1, phosphorylated focal adhesion kinase (p-FAK), and ROCK2 (fig. S3), which are essential elements for mediating mechanotransduction and have been reported to promote the osteogenic differentiation of stem cells. The staining intensities of integrin α_V and integrin β_1 in the hMSCs cultured in the Foxy5 + RGD group appeared slightly higher but were not statistically different compared with that in the RGD and Scram + RGD groups (fig. S3, A and B). The staining intensity of p-FAK in the Foxy5 + RGD group was 92 and 33% higher than those in the RGD and Scram + RGD groups, respectively (fig. S3C). Consistent with the elevated expression of focal adhesion complex components, the Foxy5 + RGD group also showed ROCK2 staining intensity 135 and 34% higher than those in the RGD and Scram + RGD groups, respectively, after 7 days of osteogenic culture (fig. S3D). This enhanced expression of p-FAK and ROCK2 supports our speculation that the Foxy5 peptide presented by the biomaterial facilitates the mechanotransduction of the cells by activating noncanonical Wnt signaling to up-regulate the expression of focal adhesion complex molecules (p-FAK) and mechanotransduction signaling molecules (ROCK2).

Foxy5 peptide immobilized on hydrogels activates RhoA signaling to enhance mechanotransduction

We next explored the molecular signaling events by which the presentation of Foxy5 peptide via the hydrogel scaffold increased the mechanotransduction and consequent osteogenic lineage commitment of hMSCs (Fig. 2A). Noncanonical Wnt5a signaling has been shown to regulate the signaling of the Rho family of GTPases, such as RhoA, and studies have shown that RhoA is essential for actin cytoskeletal stability and associated actomyosin contractility via its downstream effectors, including ROCKs (*22*). Therefore, to examine the contribution of RhoA signaling and actomyosin contractility to the osteogenic effect of Foxy5 peptide presentation, we added Y-27632, an inhibitor of ROCKs, and blebbistatin, an inhibitor of nonmuscle myosin II (NMII), to the media in the Foxy5 + RGD group during the 7 days of osteogenic culture. The inhibition of ROCK with Y-27632 completely abolished the up-regulated osteogenic gene expression

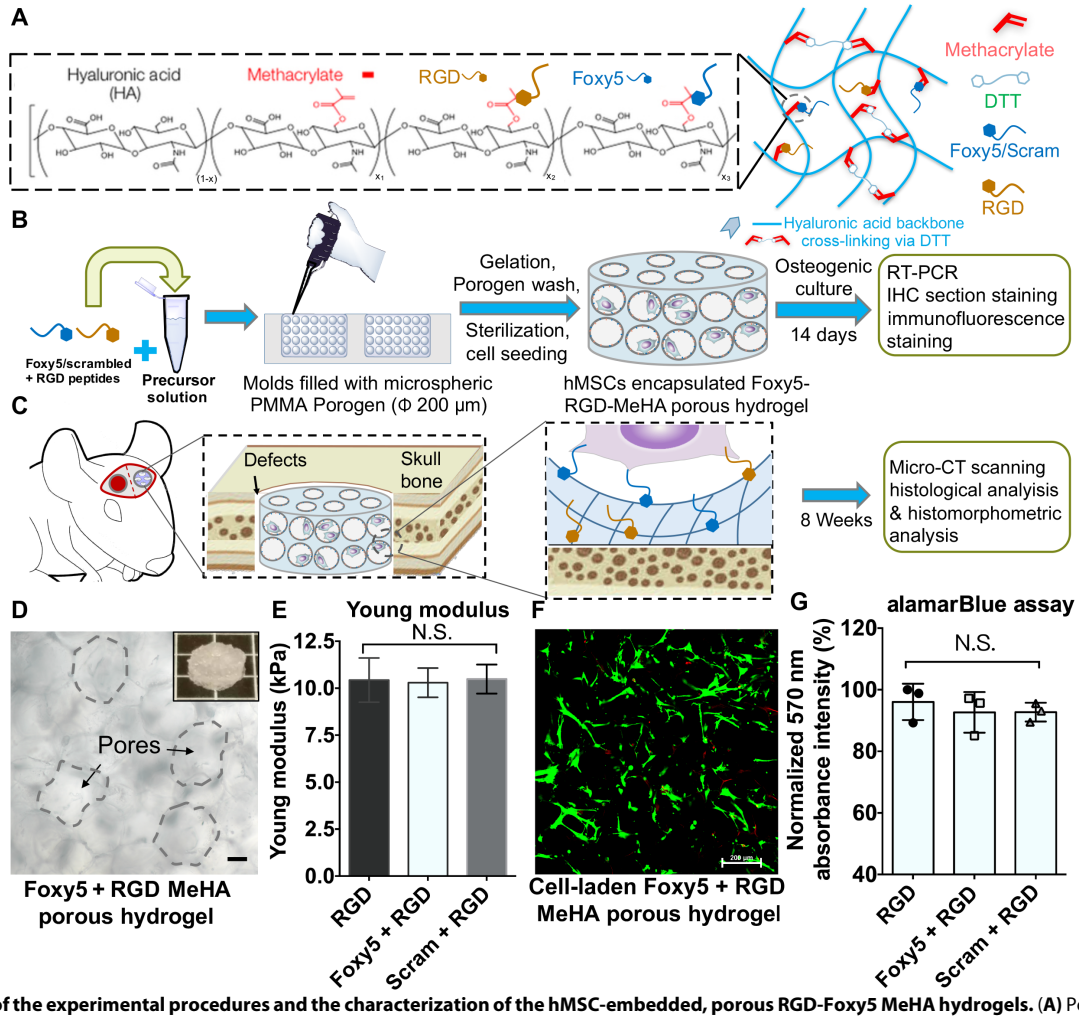

Fig. 1. Summary of the experimental procedures and the characterization of the hMSC-embedded, porous RGD-Foxy5 MeHA hydrogels. (**A**) Porous, Foxy5 + RGD peptide–conjugated MeHA hydrogels were developed by conjugating cysteine-containing functional peptides to MeHA molecules. (**B**) The porous scaffolds were used to copresent the adhesive ligand (RGD) and noncanonical Wnt5a–activating ligand (Foxy5) to synergistically induce the osteogenic lineage commitment of stem cells both in vitro and in vivo. (**C**) Rat MSC (rMSC)–seeded hydrogels were used to fill calvarial defects for regeneration. (**D**) Micrographs of the 3D porous hydrogels with Ø 200-μm pores. The inset shows the microstructure of the MeHA porous hydrogel; scale bar, 50 μm. (**E**) The Young modulus of the DTT-crosslinked MeHA hydrogels was verified using the Mach-1 mechanical tester. (**F**) The live/dead staining of the hMSCs seeded in the porous MeHA hydrogels showed the uniform distribution of the cells in the hydrogels. (**G**) Viable cell metabolic activity in the RGD, Foxy5 + RGD, and Scram + RGD hydrogels on day 7 of culture was characterized by alamarBlue assay. Data are shown as the means ± SD (n = 3).

in the Foxy5 + RGD hydrogels. Blocking NMII activity also led to significantly down-regulated expression of the osteogenic genes alkaline phosphatase (ALP), type I collagen, and osteopontin (OPN) compared with the corresponding levels in the RGD group (fig. S4). Specifically, after 7 days of osteogenic culture, the expression levels of type I collagen, ALP, RUNX2, and OPN in the Y-27632–Foxy5 + RGD group were down-regulated by 80.20, 97.96, 71.10, and 97.70%, respectively, compared with those in the Foxy5 + RGD group. The expression levels of type I collagen, ALP, RUNX2, and OPN in the blebbistatin–Foxy5 + RGD group were down-regulated by 86.23, 98.54, 24.24, and 87.48%, respectively, compared with those in the Foxy5 + RGD group. These findings suggest that the pro-osteogenic effect of the Foxy5 peptide presentation can be attributed to the activation of RhoA signaling and associated actomyosin contractility.

We further investigated the mechanism underlying the enhanced RhoA signaling and actomyosin contractility via Foxy5 peptide–mediated noncanonical Wnt signaling. Gene expression analyses revealed the up-regulated expression of Dvl2, RhoA, ROCK2, vinculin, and NMII in the presence of conjugated Foxy5 peptides after 7 days of osteogenic culture (Fig. 2B). Specifically, the Foxy5 + RGD group showed Dvl2, RhoA, ROCK2, vinculin, and NMII expression levels that were increased by 43, 27, 65, 72, and 24%, respectively, compared with those in the RGD group. Meanwhile, the expression of ROCK1, which was speculated to contribute to F-actin instability, was down-regulated by 25% in the Foxy5 + RGD group compared with that in the RGD group. Furthermore, the expression of the canonical Wnt signaling–related genes (Wnt3a, Frizzled 3, LRP5, LRP6, and β-catenin) was significantly up-regulated in the Foxy5 + RGD group compared with that in the control groups (fig. S5), and this is consistent with a previous report showing that the activated noncanonical Wnt signaling up-regulated the expression of canonical Wnt signaling factors during osteoblastogenesis (*28*). The expression of these mechanotransduction-related genes and canonical Wnt signaling–related genes in the Scram + RGD group was not

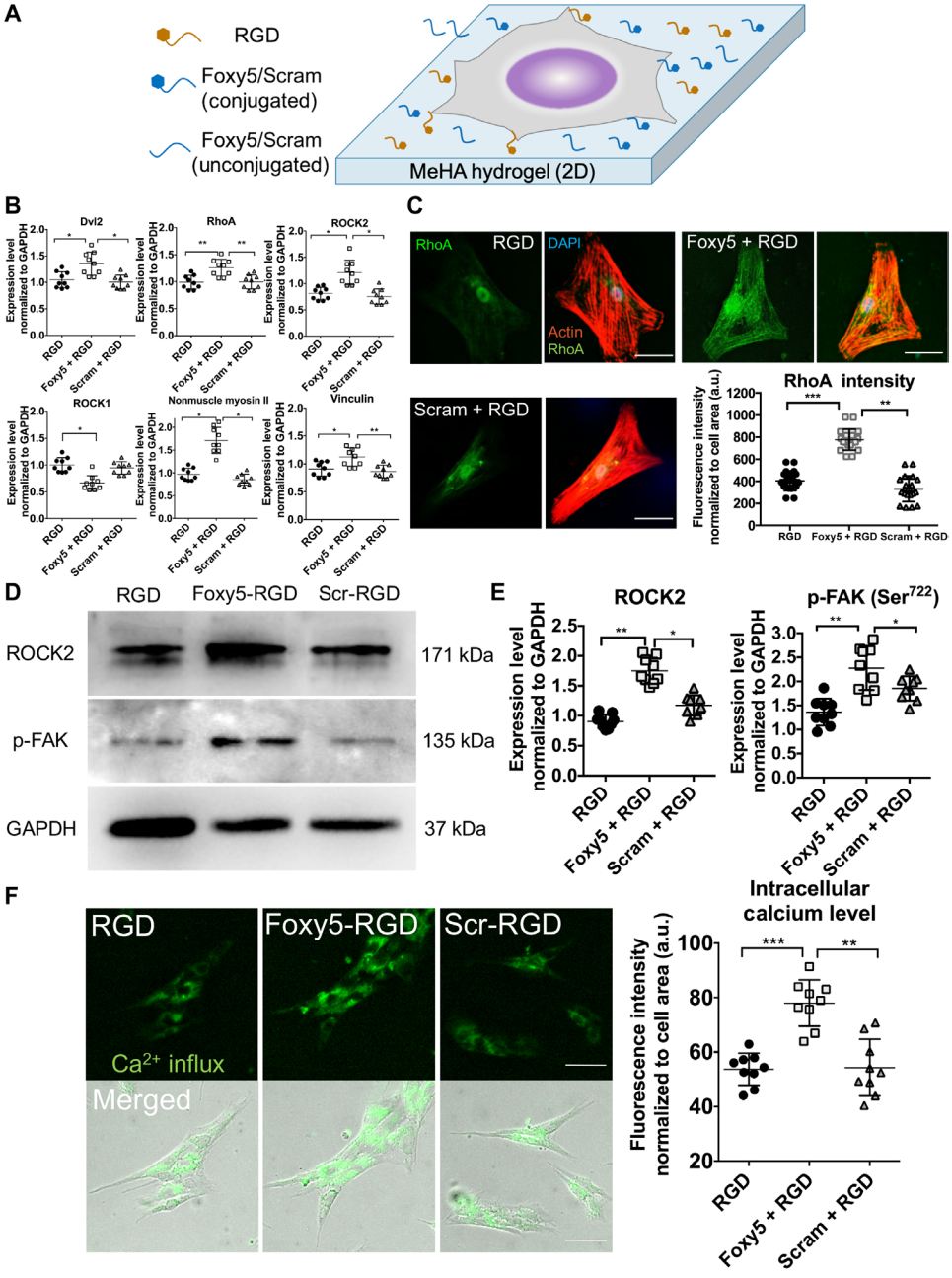

Fig. 2. Foxy5 peptide–conjugated hydrogel scaffolds activate noncanonical Wnt signaling to trigger RhoA signaling and elevate intracellular calcium. (**A**) Schematic illustration of the seeding of hMSCs on the Foxy5/Scram + RGD peptide–functionalized 2D hydrogel substrate. (**B**) Gene expression level of the RhoA signaling cascade (Wnt5a coreceptor Dvl2, RhoA, ROCK), downstream mechano-effector (NMII), and major focal adhesion adaptor protein (vinculin) in hMSCs in 3D porous hydrogels conjugated with RGD peptide alone (RGD), Foxy5 and RGD peptide (Foxy5 + RGD), or scrambled Foxy5 peptide and RGD peptide (Scram + RGD), respectively, after 7 days of osteogenic culture ($n = 9$). (**C**) Representative micrographs of fluorescence staining for F-actin (red), nuclei (blue), and RhoA (green) in hMSCs cultured on the 2D RGD, Foxy5 + RGD, and Scram + RGD hydrogels. Quantification showed a significantly higher RhoA staining intensity in the Foxy5 + RGD group than in the RGD and Scram + RGD groups ($n = 20$). a.u., arbitrary units. (**D**) Western blot bands and quantification of the expression level of mechano-responsive kinases ROCK2 and p-FAK (phosphorylated at the Ser^{722} sites) in each group (RGD, Foxy5 + RGD, Scram + RGD). (**E**) Representative merged fluorescence and bright-field micrographs of intracellular calcium in hMSCs cultured on RGD, Foxy5 + RGD, and Scram + RGD 2D hydrogels (stained with Fura-AM). (**F**) Quantification showed a significantly higher intracellular calcium level in the Foxy5 + RGD group than in the RGD and Scram + RGD groups. Scale bars, 50 μm. Data are shown as the means ± SD ($n = 9$). Statistical significance: $^{*}P < 0.05$, $^{**}P < 0.01$, and $^{***}P < 0.001$.

significantly different from that in the RGD group (Fig. 2B and fig. S5). We further quantified the expression of RhoA, ROCK2, and p-FAK based on immunofluorescence staining and Western blot analysis. The Foxy5 + RGD hydrogels showed RhoA staining intensity 92 and 134% higher than that in the RGD group and Scram + RGD groups, respectively, after 7 days of osteogenic culture (Fig. 2C). Further analysis showed a significantly increased cytoplasmic distribution of RhoA, consistent with the more prominent F-actin cytoskeleton, in

cells cultured on hydrogels conjugated with Foxy5 peptide compared with those cultured on the controls. The Western blotting results showed that the expression levels of ROCK2 and p-FAK, two key mechanotransduction signaling molecules, were significantly up-regulated in the Foxy5 + RGD hydrogels (Fig. 2D) by 83 and 75% compared with those in the RGD hydrogels, respectively, and by 39 and 35% compared with those in the Scram + RGD hydrogels, respectively (Fig. 2E). Together, these data suggest that Foxy5 peptide immobilized on hydrogels is capable of initiating noncanonical Wnt signaling via the up-regulation of Dvl2, which further activates downstream RhoA signaling, leading to enhanced F-actin stability, actomyosin contractility, and cell adhesion structure development. Furthermore, the canonical Wnt signaling has been shown to promote the osteogenesis of hMSCs directly through the up-regulation of β-catenin and downstream osteogenic genes including RUNX2, Dlx5, and Osterix (*29*). The immobilized Foxy5 peptide may indirectly facilitate the canonical Wnt signaling via the up-regulation of Frizzled3, LRP5/6, and β-catenin. More thorough examinations on the effect of Wnt5a mimetic ligands on both canonical and noncanonical Wnt signaling are certainly worthy of further investigations in the future.

Our data reveal that the Foxy5 peptide–mediated activation of noncanonical Wnt signaling is essential for regulating the expression and localization of critical signaling molecules involved in cell adhesion and mechanotransduction, including YAP, ROCK2, and p-FAK, which are essential for the osteogenesis of MSCs. The subtypes of ROCK, ROCK1, and ROCK2 have been shown to play distinct roles in regulating cytoskeletal tension. ROCK1 is a nonsecreted protein that destabilizes the actin cytoskeleton by regulating myosin light chain phosphorylation and peripheral actomyosin contraction, whereas ROCK2 is required for stabilizing the actin cytoskeleton by regulating cofilin phosphorylation (*30*). Previous studies have revealed that ROCK2 activity is effectively activated upon Wnt5a ligation to its receptors (*22*). We observed the up-regulation of ROCK2 expression and the down-regulation of ROCK1 expression, along with a significant increase in the focal adhesion levels in the MSCs presented with hydrogel-conjugated Foxy5 peptide. Therefore, the elevated ROCK2 activity results in enhanced cytoskeletal stability and more robust mechanotransduction signaling, both of which contribute to enhanced osteogenesis. When we inhibited ROCK activity in the Y-27632–Foxy5 + RGD group using 10 μM Y-27632, the expression of osteogenic genes was greatly reduced, thereby further confirming the important role of ROCK2 in Foxy5 peptide–induced osteogenesis.

Foxy5 peptide conjugated to hydrogels elevates the intracellular calcium level to promote osteogenesis

Apart from RhoA activation, noncanonical Wnt5a activation has also been reported to lead to the mobilization of free intracellular calcium, which regulates multiple cellular behaviors, including the motility and differentiation of MSCs (*31*). To test the effect of Foxy5 peptide on the intracellular calcium level, we subjected hMSCs to Fura–acetoxymethyl (AM) staining after being seeded on 2D peptide-conjugated MeHA hydrogels and cultured in osteogenic media. After 7 days of osteogenic culture, Fura-AM staining showed that cells on Foxy5 + RGD hydrogels exhibited 122 and 127% higher fluorescence intensity than those on RGD and Scram + RGD hydrogels, respectively (Fig. 2F). This finding suggests that the conjugated Foxy5 peptide is capable of activating noncanonical Wnt signaling to elevate the intracellular calcium level of MSCs, promoting osteogenesis.

Calcium-dependent noncanonical Wnt signaling pathways are known to participate in osteoblast differentiation, maturation, and bone formation (*31*, *32*). Intracellular Ca^{2+} and calcium-binding/activatable signaling factors (calmodulin, calmodulin kinase II, calcineurin, etc.) are critical to the growth and differentiation of osteoblasts (*33*). Our biochemistry analysis and histological staining further showed that the amount of bone ECM production by hMSCs was significantly enhanced together with the intracellular calcium concentration in the hydrogels conjugated with the Foxy5 peptide, and this indicates that the elevated intracellular calcium level contributes to the enhanced osteogenesis of MSCs seeded in Foxy5 peptide–functionalized hydrogels.

Presentation of immobilized Foxy5 peptide conjugated to 2D hydrogels enhances YAP/TAZ mechanosensing and RUNX2/ALP expression

The guided lineage commitment of stem cells is a critical prerequisite for successful and efficient tissue regeneration, which is known to be modulated by the concerted actions of multiple microenvironmental signals (*34*). We next examined whether the hydrogels functionalized with the Wnt5a mimetic peptide could promote the osteogenic differentiation of hMSCs. We cultured hMSCs on 2D hydrogel substrates that were functionalized with RGD alone (RGD) or RGD with either Foxy5 peptide (Foxy5 + RGD) or scrambled Foxy5 peptide (Scram + RGD) in osteogenic induction media. Supplementation of the culture media with nonconjugated soluble Foxy5 peptide was previously reported to affect the chemotaxis of cancer cells (*35*). To compare the effects of the "freely diffusing" soluble form and the hydrogel-immobilized form of Foxy5 peptide on hMSCs, we included two control groups in which the osteogenic medium was supplemented with soluble, free, nonconjugated Foxy5 or scrambled Foxy5 peptide (free Foxy5 and free Scram) in the same amounts as those present in the conjugated hydrogels (Foxy5 + RGD and Scram + RGD).

Previous studies have demonstrated the critical role of YAP/TAZ-mediated mechanotransduction signaling in osteogenesis (*36*). We performed immunofluorescence staining for YAP and RUNX2 after 7 days of osteogenic culture. The hMSCs cultured on Foxy5 + RGD hydrogels consistently exhibited more YAP nuclear localization than those in all other control groups on 2D hydrogels (Fig. 3A). Specifically, quantification of the average nuclear-to-cytoplasmic staining intensity ratio (N/C ratio) of YAP in at least 20 representative cells from each group showed that the YAP nuclear localization in the Foxy5 + RGD group was 134 and 88% higher than that in the RGD and Scram + RGD groups, respectively (Fig. 3, A and D). Moreover, the addition of soluble Foxy5 peptide in the culture media (free Foxy5) failed to significantly increase the YAP nuclear localization as much as the hydrogel-conjugated Foxy5 peptide (only a 53% increase compared with the RGD group), whereas the free, soluble scrambled peptide had no significant effect (Fig. 3, A and C). This finding indicates that the hydrogel-conjugated Foxy5 peptide has significantly higher bioactivity than the unconjugated Wnt5a peptide directly added to the media in terms of promoting mechanosensing and osteogenesis. The immobilization of this ligand on the porous scaffold greatly enhanced the local effective concentration in the microenvironment of hMSCs, thereby facilitating the ligation of Wnt5a ligands to the receptors on the cell membrane. In contrast, the direct supplementation of the ligand resulted in its dilution in the entire volume of the media and therefore reduced the local effective ligand concentration. We also speculated that

the immobilized ligands are unlikely to be internalized by cells upon ligation to membranous receptors, whereas the free ligands can be quickly internalized by cells and lose their activation function (*37*).

To examine the effect of YAP nuclear accumulation on the osteogenesis of hMSCs, we analyzed the early osteogenic lineage commitment by immunofluorescence staining for RUNX2, an essential osteogenic transcription factor, after 7 days of osteoinductive culture. Cells in the Foxy5 + RGD group showed RUNX2 nuclear-to-cytoplasmic ratio 97 and 116% greater than that in the RGD and Scram + RGD groups, consistent with the YAP nuclear localization results (Fig. 3, B and E). In contrast, the expression levels of RUNX2 in the free Foxy5 and free Scram groups were only slightly higher than those in the RGD group. Furthermore, staining for ALP, another key osteogenesis marker, showed that the average percentage of ALP-positive cells in the Foxy5 + RGD group was 55, 52, 94, and 77% higher than that in the RGD, Scram + RGD, free Foxy5, and free Scram groups, respectively (Fig. 3, C and F). These findings indicate that hydrogel-conjugated Foxy5 peptide promotes the mechanosensing-dependent osteogenic differentiation of hMSCs and that the immobilization of Foxy5 peptide on hydrogels is more effective than the continuous supplementation of media with soluble Foxy5 peptide to enhance the osteogenesis of hMSCs. To further examine the effectiveness of the immobilized Foxy5 peptide on the substrates with different stiffness, we analyzed the mechanosensing and the early osteogenic lineage commitment by immunofluorescence staining for YAP and RUNX2 on the 2D MeHA hydrogels with varying stiffness of 2, 5, and 14 kPa (*38*). Cells in the Foxy5 + RGD group showed significantly higher YAP and RUNX2 nuclear-to-cytoplasmic ratio than that in the RGD and Scram + RGD groups at each of the selected hydrogel stiffness levels (fig. S6). This indicates that the biomaterial-conjugated Foxy5 peptide promotes osteogenesis in a wide range of substrate stiffness, and we found that the pro-osteogenic effect of

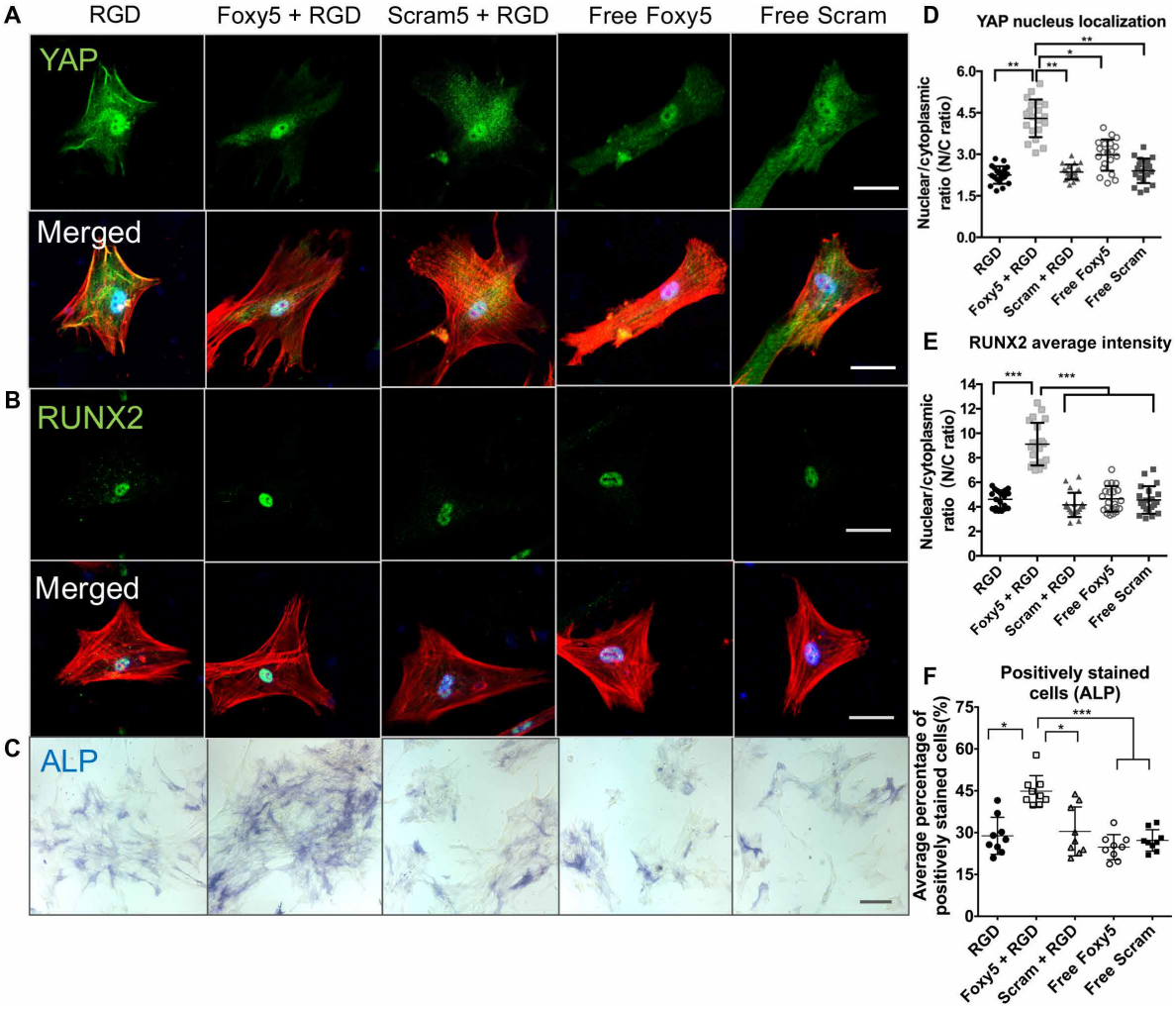

Fig. 3. Noncanonical Wnt5a mimetic peptide (Foxy5) conjugated to 2D hydrogel substrates enhances the mechanosensing and osteogenesis of hMSCs. (**A**) Fluorescence micrographs of hMSCs stained for F-actin (red), nuclei (blue), and the mechanosensing marker YAP (green) or the osteogenic marker RUNX2 (green) (**B**) and ALP (blue in bright-field) (**C**), cultured on the RGD, Foxy5 + RGD, and Scram + RGD hydrogels. (**D**) Analysis of the nuclear localization of YAP determined by the nuclear-to-cytoplasmic fluorescence intensity ratio (N/C ratio) (n = 20) and (**E**) RUNX2 nuclear localization (n = 20) and (**F**) ALP expression of representative cells cultured on 2D hydrogels in the different experimental groups (n = 9). Scale bars represent 50 μm in the fluorescence micrographs and 200 μm in the bright-field images. Data are shown as the means ± SD. Statistical significance: *P < 0.05, **P < 0.01, and ***P < 0.001 significant difference.

the conjugated Foxy5 peptide is more significant at low substrate stiffness (2 kPa) (fig. S6).

Functionalization with the Foxy5 peptide promotes hMSC osteogenic gene expression and bone matrix deposition in 3D porous hydrogels

We next examined the effect of Foxy5 peptide conjugated to 3D porous hydrogels on the osteogenic differentiation of seeded hMSCs from three different donors after 7 days (Fig. 4, A and B, fig. S7A, and tables S1 and S2) and 14 days (fig. S7B) of osteogenic culture. The real-time quantitative polymerase chain reaction (RT-qPCR) data showed that the expression levels of type I collagen, ALP, RUNX2, and OPN in cells seeded in the Foxy5 peptide–functionalized porous hydrogels (Foxy5 + RGD group) were up-regulated by 33, 57, 35, and 422%, respectively, compared with those in cells seeded in the hydrogels without Foxy5 functionalization (RGD group) (Fig. 4B)

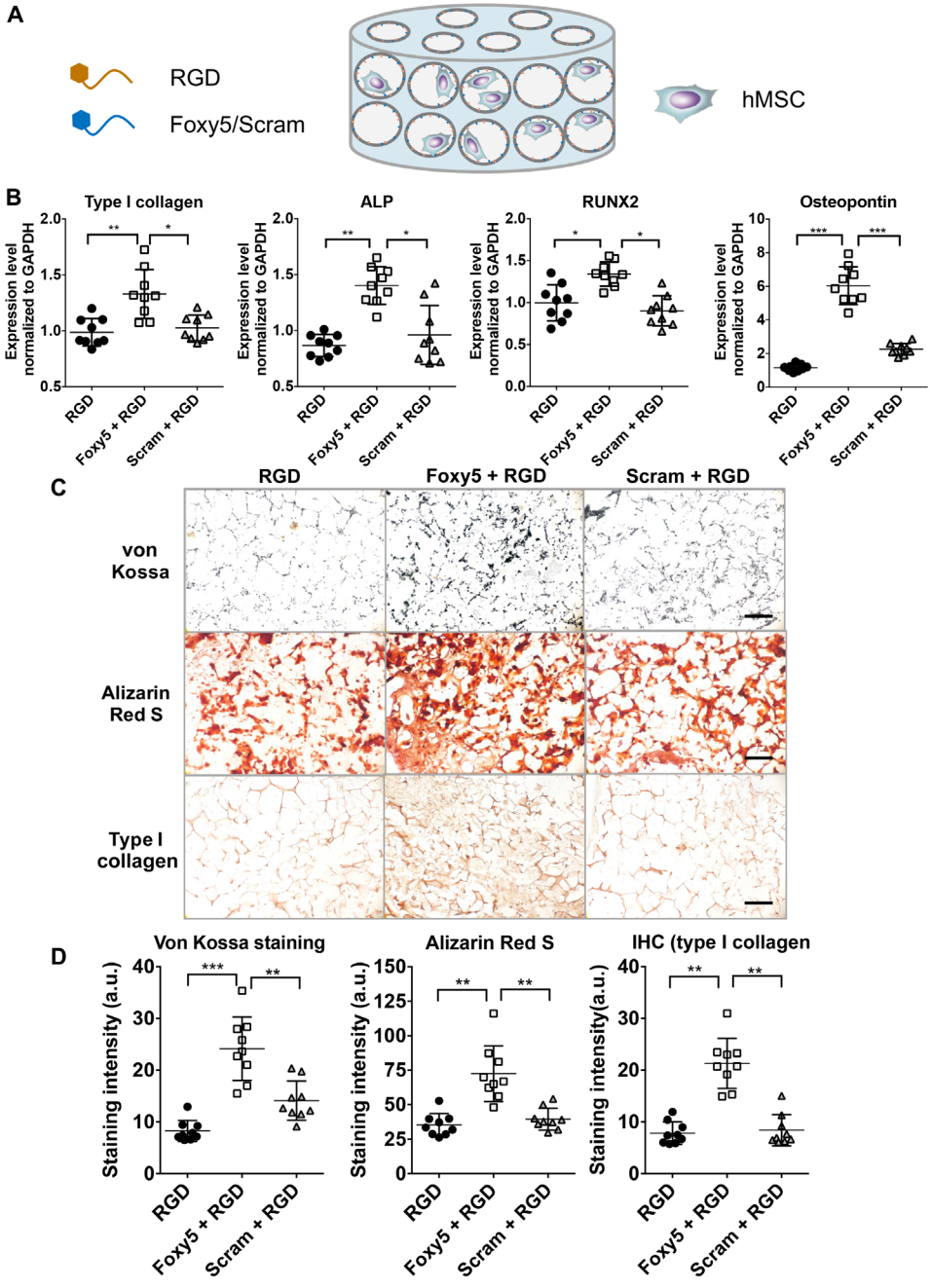

Fig. 4. Conjugating Wnt5a mimetic peptide (Foxy5) to a 3D porous hydrogel scaffold promotes hMSC osteogenic gene expression and osteogenic matrix synthesis. (**A**) Schematic illustration of the seeding of hMSCs in the Foxy5/Scram + RGD peptide–functionalized 3D hydrogel scaffolds. (**B**) Quantitative gene expression of osteogenic markers (type I collagen, RUNX2, ALP, and OPN) in hMSCs seeded in porous hydrogels conjugated with RGD peptide alone (RGD), Foxy5 and RGD peptides (Foxy5 + RGD), or Scram and RGD peptides (Scram + RGD) in osteogenic culture. (**C**) von Kossa staining, Alizarin Red S staining, and immunohistochemistry staining of type I collagen and (**D**) quantification of the staining intensities after 14 days of osteogenic culture. Scale bars, 50 μm. Data are shown as the means ± SD (n = 9). Statistical significance: * $P < 0.05$, ** $P < 0.01$, and *** $P < 0.001$.

after 7 days of osteogenic culture. In contrast, presentation of the nonfunctional scrambled peptide (Scram + RGD group) had no significant influence on the expression levels of these osteogenic genes compared with corresponding levels in the RGD group. The pro-osteogenic effect of the conjugated Foxy5 peptide diminished after 14 days of culture (fig. S7B). The diminishing effect of Foxy5 peptide can be attributed to the decreasing membrane presence of available LRP5/6 in the osteogenically differentiating hMSCs (*39*, *40*). In addition, the increasing extracellular matrix that accumulated around hMSCs over time may have also contributed to the effect of conjugated Foxy5 peptide. It is noteworthy that the declining expression of Wnt receptors and Wnt signaling are essential for the formation of mineralized matrix (*39*). Therefore, this diminished effect of Foxy5 peptide over time may be beneficial to the osteogenesis of seeded hMSCs and subsequent neobone formation. Consistent with the gene expression data, both Alizarin Red and von Kossa staining revealed more substantial calcification in the Foxy5 + RGD group than in the other control groups. Quantitative analysis showed that the Alizarin Red and von Kossa staining intensities in the Foxy5 + RGD group were 262 and 107% higher than those in the RGD groups after 14 days of culture, respectively (Fig. 4, C and D). Furthermore, we assessed the organic bone matrix synthesis of stem cells by type I collagen

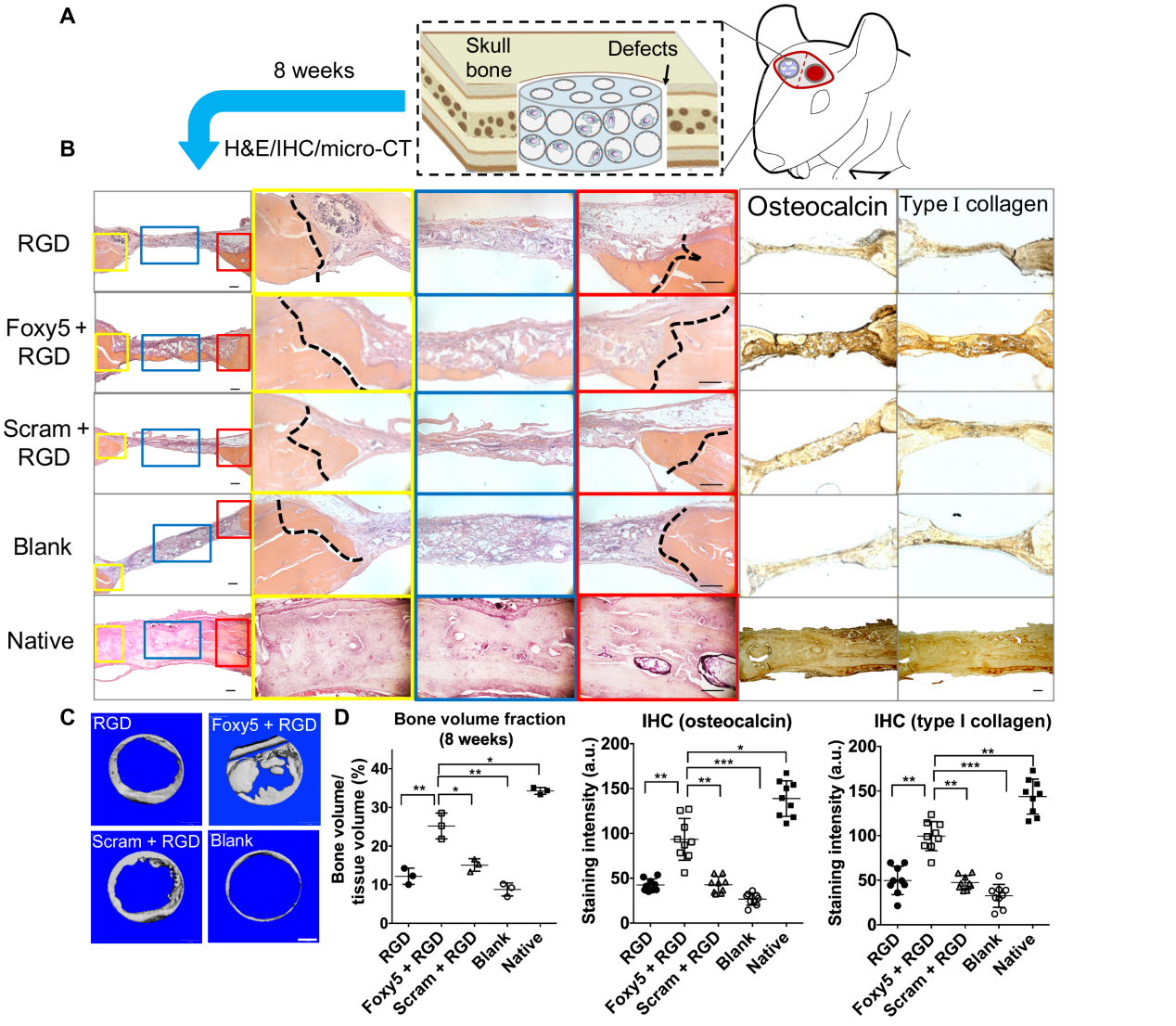

Fig. 5. Functionalization of biomaterial scaffolds with the Wnt5a mimetic peptide substantially enhances the in situ regeneration of integrated and mature bone tissues. (**A**) Schematic illustration of the implantation of rMSC-seeded and peptide-functionalized porous hydrogels in rat calvarial defects. (**B**) H&E staining and immunohistochemical staining of the native healthy bone tissue and the calvarial defects treated with the RGD hydrogels, Foxy5 + RGD hydrogels, Scram + RGD hydrogels, and no hydrogels (blank) 8 weeks after implantation ($n = 3$). High-magnification images showing the defect/native bone boundaries highlighted in yellow and red boxes and defect center areas in blue boxes in the low-magnification images of H&E-stained sections. The dotted lines indicate the boundary between the defect and native bone. The newly formed bone was seamlessly integrated with the neighboring native bone in the Foxy5 + RGD group. Scale bars, 50 μm. (**C**) Top view of 3D micro-CT images showing calvarial bone defects after 8 weeks in all groups ($n = 3$). (**D**) Bone volume (normalized to total tissue volume, BV/TV) in the calvarial defects in all groups after 8 weeks ($n = 3$). The bone volume of healthy rat calvarial bone is shown as the benchmark. Quantification of the immunohistochemical staining intensity of the osteogenic markers, including osteocalcin and type I collagen, showing the higher intensity in the Foxy5 + RGD group compared with those of the RGD and Scram + RGD control groups. Data are shown as the means ± SD ($n = 9$). Statistical significance: $^{*}P < 0.05$, $^{**}P < 0.01$, and $^{***}P < 0.001$ significant difference.

staining. The Foxy5 + RGD group exhibited 163 and 179% higher type I collagen staining than the RGD and Scram + RGD groups, respectively (Fig. 4, C and D). These findings suggest that Foxy5 conjugated to the 3D porous hydrogel scaffold significantly promotes the expression of both early- and late-stage osteogenic genes in hMSCs and inorganic/organic bone matrix synthesis.

In mature bone tissues, the unique osteoblastic microenvironment niche provides MSCs with the necessary biological cues, including stromal cell–derived factor 1, angiopoietin 1, and OPN, derived from osteoblasts, osteoclasts, osteocytes, and endothelial cells in trabecular bone and bone marrow (*19*, *41*). Many previous studies have reported the regulation of MSC signaling and lineage commitment by systemic hormones or localized growth factors (*42*). Fu *et al.* demonstrated that Wnt3a-mediated canonical Wnt signaling activation antagonizes the terminal osteogenic differentiation of MSCs, while Wnt5a-mediated noncanonical Wnt signaling mitigates the inhibitory effect of Wnt3a. In the natural osteoblastic niche, Wnt5a proteins are secreted by the surrounding tissues and bind to the Frizzled/Ror2 surface Wnt receptors of hMSCs via paracrine mechanisms (*43*). We used porous hydrogels functionalized with Wnt5a mimetic Foxy5 peptide to emulate this pro-osteogenic niche and promote the osteogenesis of hMSCs. In addition to Foxy5 peptide, RGD peptide was also conjugated to all hydrogels to provide adhesive motifs for the hMSCs because Foxy5 peptide alone cannot support effective cell adhesion. The promechanotransduction and pro-osteogenic effects of Foxy5 peptide were therefore not studied in the absence of RGD peptides, which is a limitation of the study. Nevertheless, integrin ligands are important components of the natural osteogenic niche in bones. The potential crosstalk between integrin signaling and Wnt signaling and the associated effects on stem cell differentiation certainly warrant further investigation.

Efficacy of the MeHA–Foxy5 + RGD scaffold for calvarial defect repair in rats by activating noncanonical Wnt5a signaling

We further evaluated the efficacy of the Foxy5 peptide conjugated to the hydrogel in assisting in vivo bone regeneration in rat calvarial defects. Rat MSCs (rMSCs) with trilineage differentiation potential (*44*–*46*) were first seeded in porous hydrogels functionalized with RGD, Foxy5 + RGD, or Scram + RGD peptides and cultured in osteogenic media for 7 days prior to transplantation into the defects (Fig. 5A). The RT-qPCR data showed that the expression levels of type I collagen, ALP, RUNX2, OPN, Dvl2, RhoA, and vinculin in rMSCs of the Foxy5 + RGD group were all significantly higher compared with those in the control groups (RGD group, Scram + RGD) after 7 days of osteogenic culture (fig. S8, A and B). Eight weeks after transplantation, both hematoxylin and eosin (H&E) staining and immunohistochemical staining for osteocalcin and type I collagen revealed enhanced osteoblastic marker expression and bone matrix formation in the Foxy5 + RGD group compared with the RGD, Scram + RGD, and blank groups (Fig. 5B). The average staining intensity for osteocalcin was 124, 114, and 240% higher and that of type I collagen was 105, 104, and 144% higher in the Foxy5 + RGD group than in the blank, RGD, and Scram + RGD groups, respectively (Fig. 5D). The average staining intensity for osteocalcin and type I collagen in the Foxy5 + RGD group was still around 30% lower than that in the native calvarial tissue (Fig. 5D). Furthermore, the microcomputed tomography (micro-CT) reconstruction data revealed considerably more new bone formation in the defects treated with hydrogels conjugated with Foxy5 and RGD peptides (Foxy5 + RGD group) than in those treated with the control hydrogels (blank, RGD, and Scram + RGD groups) (Fig. 5C). Quantitative analysis showed that the bone volume–to–total tissue volume (BV/TV) ratio in the Foxy5 + RGD group was 107, 57, and 198% higher than that in the RGD, Scram + RGD, and sham blank groups, respectively. Notably, the average BV/TV ratio of healthy calvarial bone was determined to be 35.25% due to other skeletal components, such as fibrous connective tissues. The average BV/TV ratio in the Foxy5 + RGD group was 25.19%, suggesting a substantial recovery of approximately 71.49% of the healthy calvarial bone volume. These findings demonstrate that the functionalization of biomaterial scaffolds with this Wnt5a mimetic peptide can substantially enhance bone regeneration in vivo. No significant abnormalities in tissue structure or morphology were observed around the implantation site. We believe that the restricted bioactivity of the mimetic peptide (compared with that of the parent protein) and the immobilization of this Wnt5a ligand on the biomaterial for local implantation will limit potential undesired nonspecific actions that may arise due to peptide transportation to other "off-target" sites (*47*).

CONCLUSION

In this study, we demonstrate that the HA hydrogels functionalized with the noncanonical Wnt5a mimic peptide Foxy5 promote mechanotransduction and the osteogenic commitment of residing hMSCs by mimicking the pro-osteogenic microenvironment within

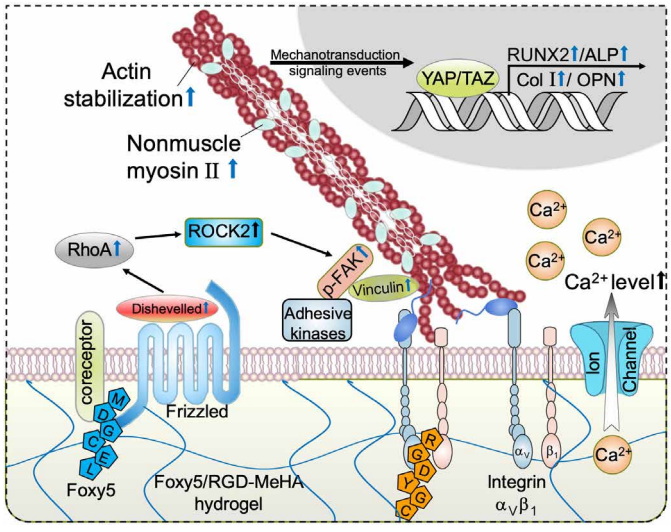

Fig. 6. Schematic illustration of the Wnt5a mimetic peptide–conjugated, porous HA hydrogels promoting the osteogenesis of seeded hMSCs by activating RhoA signaling and elevating the intracellular calcium level. Presentation of the Wnt5a mimetic Foxy5 peptide by the hydrogel scaffold to Wnt receptors (Frizzled) and coreceptors on the membrane of seeded MSCs activates noncanonical Wnt signaling, leading to the activation of Dvl2 and downstream RhoA-ROCK2 signaling. The activation of RhoA signaling leads to enhanced cytoskeletal stability and actomyosin contractility (increased NMII) and therefore boosts mechanotransduction and the formation of focal adhesions (elevated vinculin expression). Meanwhile, the presentation of Foxy5 peptide mediates elevated intracellular calcium levels, contributing to the amplification of mechanosensing and osteogenic lineage commitment. The amplified mechanosensing of hMSCs residing in Foxy5 peptide–functionalized hydrogels is demonstrated by the increased YAP nuclear localization and up-regulated RhoA and ROCK2 expression, and these events promote the commitment of MSCs to the osteogenic lineage in the synthetic osteogenic niche microenvironment.

trabecular bone. Our data show that the Wnt5a mimic peptide conjugated to the biomaterial scaffold enhances activation of the noncanonical Wnt signaling pathway involving RhoA-ROCKs, thereby promoting mechanotransduction and the osteogenesis of hMSCs (Fig. 6). Our findings shed light on the significance of the biofunctionalization of biomaterials for regenerative medicine applications.

MATERIALS AND METHODS

Synthesis of MeHA and porous hydrogel fabrication

MeHA macromolecules were synthesized from sodium hyaluronate powder (molecular weight, ~74 kDa; Lifecore, Chaska, Minnesota, USA), as previously reported (*8*). Briefly, 100 ml of 1% (w/v) sodium hyaluronate solution was reacted for 24 hours with 4 or 1.5 ml of methacrylic anhydride at pH 9.5, adjusted with 2 M NaOH solution. After complete dialysis and lyophilization, 100% methacrylation or 30% methacrylation was confirmed using proton nuclear magnetic resonance (^{1}H NMR). The RGD peptide (GCGYGRGDSPG) and Foxy5 peptide (MDGCEL) (GenScript, Nanjing, Jiangsu, China) with a cysteine amino acid at the C-terminal end were conjugated to the MeHA backbone with a Michael addition reaction between the methacrylate groups and the thiol groups of each peptide in basic phosphate buffer (pH 8.0) containing 10 μM tris(2-carboxyethyl) phosphine at 37°C. The molar ratio of methacrylate to each peptide thiol was 100:3. RGD-functionalized, Foxy5-conjugated porous MeHA hydrogels were fabricated from 50 μl of the peptide-conjugated MeHA solution (3% w/v, 100% methacrylation) after 2 hours, with 1.51 μmol of DTT as the cross-linker to consume all residual methacrylic groups, in round polyvinyl chloride molds fully packed with a poly(methyl methacrylate) (PMMA) microsphere porogen (Ø 200 μm). The constructs generated were immersed in acetone and shaken at 90 rpm to dissolve the PMMA porogen, sterilized with 75% ethanol for 1 day, and rinsed three times with sterile phosphate-buffered saline (PBS). In the directly Foxy5 peptide–supplemented MeHA (free Foxy5) group and the directly scrambled peptide–supplemented MeHA (free Scram) group, we only used the same Foxy5 + RGD–functionalized MeHA solution or Scram + RGD–functionalized MeHA solution (3% w/v, 100% methacrylation) to fabricate the porous hydrogels, respectively.

We used MeHA with 30% methacrylation supplemented with 0.05% (w/v) photoinitiator I2959 (Sigma-Aldrich, MO, USA) to make Foxy5 + RGD–functionalized MeHA solution, Scram + RGD–functionalized MeHA solution, or RGD-functionalized MeHA solution (3% w/v, 30% methacrylation) and to fabricate 2D hydrogels with different stiffness in polyvinyl chloride molds under 367, 467, 667, or 1067 seconds of UV exposure. All 2D hydrogels were sterilized before cell culture. The surface roughness and modulus were determined by atomic force microscopy (Bruker, MA, USA).

2D-biofunctionalized substrates were fabricated by polymerizing peptide-conjugated MeHA precursor solutions (3% w/v, 30% methacrylation) under UV light (wavelength, 365 nm; intensity, 7 mW/cm^2) on methacrylated glass coverslips. The porous MeHA hydrogel constructs (height, ~1.5 mm; Ø 1 mm) were polymerized in molds filled with Ø 200-μm PMMA microbeads to form an interconnected porous structure for in vitro experiments and for in vivo calvarial defect regeneration (Fig. 1, B and C) (*9*). Homogenous, interconnected spherical structures within the hydrogels were characterized through bright-field images captured using a fluorescence microscope (Nikon, Japan) (Fig. 1D). The Young moduli of the hydrogels were determined using a mechanical tester (Mach-1, Biomomentum Inc., Suite, Canada), and the strain-controlled frequency sweep mechanical tests were performed using a rheometer (Malvern Inc., Malvern, Britain).

Cell culture and osteogenic differentiation

Passage-4 hMSCs (Lonza, Walkersville, Maryland, USA) were expanded in basal growth medium [α-minimal essential medium (MEM) supplemented with 16.7% (v/v) fetal bovine serum (FBS), penicillin-streptomycin (P/S; 100 U ml^{-1}), and 2 mM L-glutamine]. Growth medium (50 μl) containing 5×10^5 hMSCs (10^8 cells ml^{-1}) was injected into one semidry, porous MeHA-RGD hydrogel, which was incubated at 37°C for 4 hours to allow cell attachment to the hydrogels. Then, 1 ml of osteogenic medium [α-MEM, 16.67% FBS, 1% P/S, 2 mM L-glutamine, 10 mM β-glycerophosphate disodium, L-ascorbic acid 2-phosphate (50 mg ml^{-1}), and 100 nM dexamethasone] was added to all the hydrogels, and the medium was changed every 2 days. In the control group, Foxy5 peptide or scrambled peptide solution was added directly to the hydrogels at the beginning of osteogenic culture. Samples were collected on days 7 and 14 to evaluate the degree of osteogenesis by traditional qPCR and immunofluorescence staining. Cell viability was determined by alamarBlue assay (Invitrogen, Carlsbad, California, USA) after 7 days in osteogenic culture. Live/dead staining was performed by adding 3 μM calcein AM and 3 μM propidium iodide (Thermo Fisher Scientific, Waltham, Massachusetts, USA) to the hydrogels. After incubation for 30 min at 37°C, the hydrogels were washed three times with PBS, and fluorescence images were captured using a confocal microscope (Nikon C2, Tokyo, Japan). The quantification of immunofluorescence staining results was conducted by using the ImageJ software [National Institutes of Health (NIH), Baltimore, Maryland, USA]. First, we adjusted the color images of the immunofluorescence staining to the 8-bit grayscale images, and then we selected the region of cells that best represent the overall staining intensity of the samples in the immunofluorescence staining results. The average grayscale values of the region of interest taken from at least 20 cells in each group were determined and compared to get the quantification results. The reported data of biochemical assays are the pooled results from three experiments.

Gene expression analysis with RT-qPCR

All samples were homogenized in 1 ml of TRIzol reagent (Invitrogen), and total RNA was extracted according to the manufacturer's protocol. The RNA concentration was measured using a NanoDrop One spectrophotometer (NanoDrop Technologies, Waltham, Massachusetts, USA). Total RNA (1 μg) was reverse transcribed into cDNA using the RevertAid First Strand cDNA Synthesis Kit (Thermo Fisher Scientific). qPCR was performed on an Applied Biosystems StepOnePlus Real-Time PCR System with TaqMan primers and probes (Applied Biosciences, Waltham, Massachusetts, USA) specific for glyceraldehyde 3-phosphate dehydrogenase (GAPDH) and other osteogenic genes, including those encoding RUNX2, ALP, and type I collagen. The sequences of the TaqMan primers and probes used are listed in table S2. The osteogenic gene expression levels were normalized to that of GAPDH, and the relative expression levels were calculated with the $2^{-\Delta\Delta Ct}$ method.

Histological assessment of osteogenic markers in vitro

Hydrogel samples were fixed overnight in 4% paraformaldehyde at 4°C, dehydrated in a graded series of ethanol, crystalized in a graded series of xylene, and embedded in paraffin. Histological sections (7 μm) were stained for type I collagen using the VECTASTAIN ABC Kit and the DAB Substrate Kit (Vector Laboratories, Burlingame,

California, USA). Briefly, hyaluronidase (0.5 g liter^{-1}) was applied to the rehydrated samples to predigest them at 37°C for 30 min. The samples were then incubated with 0.5 N acetic acid for 4 hours at 4°C to induce swelling, followed by incubation at 4°C overnight with a primary antibody directed against type I collagen (anti–type I collagen, diluted 1:200; sc-59772, Santa Cruz Biotechnology). Immunofluorescence staining for the osteogenic-related proteins (YAP and RUNX2) and cellular contraction–related proteins (RhoA) was conducted as previously reported (*9*). The calcification of phosphates and calcium ions was identified with von Kossa staining and Alizarin Red S staining, respectively. Briefly, von Kossa stain was applied to the rehydrated sections, as previously reported. To stain with Alizarin Red S, 1 ml of 0.5% (w/v) Alizarin Red S solution (Sigma) was applied to each hydrogel sample; the samples were then incubated for 5 min at room temperature before being washed, dehydrated, cleared, and sealed. Images were captured using a bright-field microscope (Nikon). The quantification was conducted by using the ImageJ software (NIH). First, we adjusted the color images of immunohistochemistry (IHC) staining to the 8-bit grayscale images, and then we selected regions of interests of identical size that best represent the overall staining intensity of the samples in the IHC staining results. The average grayscale values of the region of interest taken from three parallel samples in each group were determined and compared to get the quantification results. The reported data of biochemical assays are pooled results from three experiments.

In vivo calvarial defect repair and histological assessment

Strictly following the guidelines of the Institutional Animal Care and Use Committee at The Chinese University of Hong Kong, 12-week-old male Sprague-Dawley rats were randomly divided into four groups, shaved, and prepped for aseptic surgery. A midline skin flap was raised over the parietal bones and reflected caudally to expose the midsagittal and transverse sutures. The periosteum was incised along the midsagittal suture and the right or left transverse suture and removed to expose the parietal bone. A 5-mm-diameter defect was created using a trephine with normal saline irrigation during processing, and a section of the bone was removed to expose the dura mater. 3D porous peptide–functionalized HA hydrogels (n = 3 per group) 5 mm in diameter and 1 mm thick were seeded with 1 million rMSCs with trilineage differentiation potential (*46*). After 7 days of in vitro osteogenic induction in the incubator, the hydrogels were implanted into the calvarial defects. All experimental animals were maintained until 8 weeks from the day of defect creation. After the rats were euthanized, the parietal bones were harvested and decalcified with 10% EDTA solution. The subsequent H&E staining and histological analysis were performed as described in previous publications (*9*).

Statistical analysis

All data are presented as the means ± SD. Statistica (Statsoft, Tulsa, Oklahoma, USA) was used to perform the statistical analyses using two-way analysis variance (ANOVA) and Tukey's honest significant difference post hoc test of the means; the culture period and experimental groups were used as independent variables.

SUPPLEMENTARY MATARIALS

Supplementary material for this article is available at http://advances.sciencemag.org/cgi/content/full/5/10/eaaw3896/DC1

Fig. S1. Characterization of the methacrylated hyaluronic acid (MeHA) macromers.
Fig. S2. The mechanical characterizations of the MeHA hydrogels conjugated with various groups of peptide.
Fig. S3. Foxy5 peptide-conjugated hydrogels upregulate the expression of mechanotransduction signaling molecules in the seeded hMSCs.
Fig. S4. The promoting effect of conjugated Foxy5 peptide on the osteogenesis of hMSCs is dependent on ROCK and non-muscle myosin II activities.
Fig. S5. Conjugated Foxy5 peptides enhance the expression of canonical Wnt-related genes of hMSCs seeded in the 3D hydrogel.
Fig. S6. The hydrogel-conjugated Foxy5 peptide promotes the osteogenesis in a wide range of hydrogel substrate stiffness.
Fig. S7. The conjugated Foxy5 peptide promotes the osteogenesis of the hMSCs from multiple donors.
Fig. S8. The conjugated Foxy5 peptide promotes the mechanotransduction and osteogenesis of the seeded rMSCs.
Table S1. The sequence of the primers and probes used for real-time PCR are listed.
Table S2. The donor information of the hMSCs used for the in vitro experiments is listed.

View/request a protocol for this paper from *Bio-protocol*.

REFERENCES AND NOTES

1. S. Zeitouni, U. Krause, B. H. Clough, H. Halderman, A. Falster, D. T. Blalock, C. D. Chaput, H. W. Sampson, C. A. Gregory, Human mesenchymal stem cell–derived matrices for enhanced osteoregeneration. *Sci. Transl. Med.* **4**, 132ra155 (2012).
2. D. Toscani, M. Bolzoni, F. Accardi, F. Aversa, N. Giuliani, The osteoblastic niche in the context of multiple myeloma. *Ann. N.Y. Acad. Sci.* **1335**, 45–62 (2015).
3. J. M. Oliveira, L. Carvalho, J. Silva-Correia, S. Vieira, M. Majchrzak, B. Lukomska, L. Stanaszek, P. Strymecka, I. Malysz-Cymborska, D. Golubczyk, L. Kalkowski, R. L. Reis, M. Janowski, P. Walczak, Hydrogel-based scaffolds to support intrathecal stem cell transplantation as a gateway to the spinal cord: Clinical needs, biomaterials, and imaging technologies. *NPJ Regen. Med.* **3**, 8 (2018).
4. A. E. Jakus, A. L. Rutz, S. W. Jordan, A. Kannan, S. M. Mitchell, C. Yun, K. D. Koube, S. C. Yoo, H. E. Whiteley, C. P. Richter, R. D. Galiano, W. K. Hsu, S. R. Stock, E. L. Hsu, R. N. Shah, Hyperelastic "bone": A highly versatile, growth factor–free, osteoregenerative, scalable, and surgically friendly biomaterial. *Sci. Transl. Med.* **8**, 358ra127 (2016).
5. L. R. Carpio, E. W. Bradley, M. E. McGee-Lawrence, M. M. Weivoda, D. D. Poston, A. Dudakovic, M. Xu, T. Tchkonia, J. L. Kirkland, A. J. van Wijnen, M. J. Oursler, J. J. Westendorf, Histone deacetylase 3 supports endochondral bone formation by controlling cytokine signaling and matrix remodeling. *Sci. Signal.* **9**, ra79 (2016).
6. R. Li, J. Li, J. Xu, D. S. Hong Wong, X. Chen, W. Yuan, L. Bian, Multiscale reconstruction of a synthetic biomimetic micro-niche for enhancing and monitoring the differentiation of stem cells. *Biomaterials* **173**, 87–99 (2018).
7. J. J. Green, J. H. Elisseeff, Mimicking biological functionality with polymers for biomedical applications. *Nature* **540**, 386–394 (2016).
8. L. Bian, M. Guvendiren, R. L. Mauck, J. A. Burdick, Hydrogels that mimic developmentally relevant matrix and N-cadherin interactions enhance MSC chondrogenesis. *Proc. Natl. Acad. Sci. U.S.A.* **110**, 10117–10122 (2013).
9. M. Zhu, S. Lin, Y. Sun, Q. Feng, G. Li, L. Bian, Hydrogels functionalized with N-cadherin mimetic peptide enhance osteogenesis of hMSCs by emulating the osteogenic niche. *Biomaterials* **77**, 44–52 (2015).
10. C. Zhao, A. Ichimura, N. Qian, T. Iida, D. Yamazaki, N. Noma, M. Asagiri, K. Yamamoto, S. Komazaki, C. Sato, F. Aoyama, A. Sawaguchi, S. Kakizawa, M. Nishi, H. Takeshima, Mice lacking the intracellular cation channel TRIC-B have compromised collagen production and impaired bone mineralization. *Sci. Signal.* **9**, ra49 (2016).
11. Z. Steinhart, S. Angers, Wnt signaling in development and tissue homeostasis. *Development* **145**, dev146589 (2018).
12. J. Luther, T. A. Yorgan, T. Rolvien, L. Ulsamer, T. Koehne, N. Liao, D. Keller, N. Vollersen, S. Teufel, M. Neven, S. Peters, M. Schweizer, A. Trumpp, S. Rosigkeit, E. Bockamp, S. Mundlos, U. Kornak, R. Oheim, M. Amling, T. Schinke, J. P. David, Wnt1 is an Lrp5-independent bone-anabolic Wnt ligand. *Sci. Transl. Med.* **10**, eaau7137 (2018).
13. R. Baron, M. Kneissel, WNT signaling in bone homeostasis and disease: From human mutations to treatments. *Nat. Med.* **19**, 179–192 (2013).
14. S. Uehara, N. Udagawa, H. Mukai, A. Ishihara, K. Maeda, T. Yamashita, K. Murakami, M. Nishita, T. Nakamura, S. Kato, Y. Minami, N. Takahashi, Y. Kobayashi, Protein kinase N3 promotes bone resorption by osteoclasts in response to Wnt5a-Ror2 signaling. *Sci. Signal.* **10**, eaan0023 (2017).
15. K. Maeda, Y. Kobayashi, N. Udagawa, S. Uehara, A. Ishihara, T. Mizoguchi, Y. Kikuchi, I. Takada, S. Kato, S. Kani, M. Nishita, K. Marumo, T. J. Martin, Y. Minami, N. Takahashi, Wnt5a-Ror2 signaling between osteoblast-lineage cells and osteoclast precursors enhances osteoclastogenesis. *Nat. Med.* **18**, 405–412 (2012).
16. A. Kikuchi, H. Yamamoto, A. Sato, S. Matsumoto, Wnt5a: Its signalling, functions and implication in diseases. *Acta Physiol.* **204**, 17–33 (2012).
17. Z. Li, K. Zhang, X. Li, H. Pan, S. Li, F. Chen, J. Zhang, Z. Zheng, J. Wang, H. Liu, Wnt5a suppresses inflammation-driven intervertebral disc degeneration via a TNF-α/NF-κB–Wnt5a negative-feedback loop. *Osteoarthr. Cartil.* **26**, 966–977 (2018).

18. K. C. Keller, H. Ding, R. Tieu, N. R. L. Sparks, D. D. Ehnes, N. I. zur Nieden, Wnt5a supports osteogenic lineage decisions in embryonic stem cells. *Stem Cells Dev.* **25**, 1020–1032 (2016).
19. S. J. Morrison, D. T. Scadden, The bone marrow niche for haematopoietic stem cells. *Nature* **505**, 327–334 (2014).
20. A. Briolay, P. Lencel, L. Bessueille, J. Caverzasio, R. Buchet, D. Magne, Autocrine stimulation of osteoblast activity by Wnt5a in response to TNF-α in human mesenchymal stem cells. *Biochem. Biophys. Res. Commun.* **430**, 1072–1077 (2013).
21. E. Nemoto, Y. Ebe, S. Kanaya, M. Tsuchiya, T. Nakamura, M. Tamura, H. Shimauchi, Wnt5a signaling is a substantial constituent in bone morphogenetic protein-2-mediated osteoblastogenesis. *Biochem. Biophys. Res. Commun.* **422**, 627–632 (2012).
22. A. Santos, A. D. Bakker, J. M. A. de Blieck-Hogervorst, J. Klein-Nulend, WNT5A induces osteogenic differentiation of human adipose stem cells via rho-associated kinase ROCK. *Cytotherapy* **12**, 924–932 (2010).
23. N. D. Bade, R. D. Kamien, R. K. Assoian, K. J. Stebe, Curvature and Rho activation differentially control the alignment of cells and stress fibers. *Sci. Adv.* **3**, e1700150 (2017).
24. C. E. Ford, E. J. Ekström, J. Howlin, T. Andersson, Retracted manuscript: The WNT-5a derived peptide, Foxy-5, possesses dual properties that impair progression of ERα negative breast cancer. *Cell Cycle* **8**, 1838–1842 (2011).
25. L. M. Mehdawi, C. P. Prasad, R. Ehrnström, T. Andersson, A. Sjölander, Non-canonical WNT5A signaling up-regulates the expression of the tumor suppressor 15-PGDH and induces differentiation of colon cancer cells. *Mol. Oncol.* **10**, 1415–1429 (2016).
26. B. Guo, B. Lei, P. Li, P. X. Ma, Functionalized scaffolds to enhance tissue regeneration. *Regen. Biomater.* **2**, 47–57 (2015).
27. D. R. Lemos, J. S. Duffield, Tissue-resident mesenchymal stromal cells: Implications for tissue-specific antifibrotic therapies. *Sci. Transl. Med.* **10**, eaan5174 (2018).
28. M. Okamoto, N. Udagawa, S. Uehara, K. Maeda, T. Yamashita, Y. Nakamichi, H. Kato, N. Saito, Y. Minami, N. Takahashi, Y. Kobayashi, Noncanonical Wnt5a enhances Wnt/β-catenin signaling during osteoblastogenesis. *Sci. Rep.* **4**, 4493 (2014).
29. T. Gaur, C. J. Lengner, H. Hovhannisyan, R. A. Bhat, P. V. N. Bodine, B. S. Komm, A. Javed, A. J. van Wijnen, J. L. Stein, G. S. Stein, J. B. Lian, Canonical WNT signaling promotes osteogenesis by directly stimulating Runx2 gene expression. *J. Biol. Chem.* **280**, 33132–33140 (2005).
30. J. Shi, X. Wu, M. Surma, S. Vemula, L. Zhang, Y. Yang, R. Kapur, L. Wei, Distinct roles for ROCK1 and ROCK2 in the regulation of cell detachment. *Cell Death Dis.* **4**, e483 (2013).
31. T. P. Yamaguchi, A. Bradley, A. P. McMahon, S. Jones, A Wnt5a pathway underlies outgrowth of multiple structures in the vertebrate embryo. *Development* **126**, 1211–1223 (1999).
32. R. A. Surmenev, M. A. Surmeneva, A. A. Ivanova, Significance of calcium phosphate coatings for the enhancement of new bone osteogenesis–A review. *Acta Biomater.* **10**, 557–579 (2014).
33. M. Zayzafoon, Calcium/calmodulin signaling controls osteoblast growth and differentiation. *J. Cell. Biochem.* **97**, 56–70 (2006).
34. A. W. Duncan, F. M. Rattis, L. N. DiMascio, K. L. Congdon, G. Pazianos, C. Zhao, K. Yoon, J. M. Cook, K. Willert, N. Gaiano, T. Reya, Integration of Notch and Wnt signaling in hematopoietic stem cell maintenance. *Nat. Immunol.* **6**, 314–322 (2005).
35. A. Säfholm, K. Leandersson, J. Dejmek, C. K. Nielsen, B. O. Villoutreix, T. Andersson, A formylated hexapeptide ligand mimics the ability of Wnt-5a to impair migration of human breast epithelial cells. *J. Biol. Chem.* **281**, 2740–2749 (2006).
36. J.-X. Pan, L. Xiong, K. Zhao, P. Zeng, B. Wang, F.-L. Tang, D. Sun, H.-h. Guo, X. Yang, S. Cui, W.-F. Xia, L. Mei, W.-C. Xiong, YAP promotes osteogenesis and suppresses adipogenic differentiation by regulating β-catenin signaling. *Bone Res.* **6**, 18 (2018).
37. K. A. Kilian, M. Mrksich, Directing stem cell fate by controlling the affinity and density of ligand–receptor interactions at the biomaterials interface. *Angew. Chem.* **124**, 4975–4979 (2012).
38. B. D. Cosgrove, K. L. Mui, T. P. Driscoll, S. R. Caliari, K. D. Mehta, R. K. Assoian, J. A. Burdick, R. L. Mauck, N-cadherin adhesive interactions modulate matrix mechanosensing and fate commitment of mesenchymal stem cells. *Nat. Mater.* **15**, 1297–1306 (2016).
39. G. Van Der Horst, S. M. van der Werf, H. Farih-Sips, R. L. van Bezooijen, C. W. Löwik, M. Karperien, Downregulation of Wnt signaling by increased expression of Dickkopf-1 and -2 is a prerequisite for late-stage osteoblast differentiation of KS483 cells. *J. Bone Miner. Res.* **20**, 1867–1877 (2005).
40. J. Bao, J. J. Zheng, D. Wu, The structural basis of DKK-mediated inhibition of Wnt/LRP signaling. *Sci. Signal.* **5**, pe22 (2012).
41. T. Yin, L. Li, The stem cell niches in bone. *J. Clin. Invest.* **116**, 1195–1201 (2006).
42. M. S. Rahman, N. Akhtar, H. M. Jamil, R. S. Banik, S. M. Asaduzzaman, TGF-β/BMP signaling and other molecular events: Regulation of osteoblastogenesis and bone formation. *Bone Res.* **3**, 15005 (2015).
43. H.-D. Fu, B.-K. Wang, Z.-Q. Wan, H. Lin, M.-L. Chang, G.-L. Han, Wnt5a mediated canonical Wnt signaling pathway activation in orthodontic tooth movement: Possible role in the tension force-induced bone formation. *J. Mol. Histol.* **47**, 455–466 (2016).
44. S. Lin, W. Y. W. Lee, Q. Feng, L. Xu, B. Wang, G. C. W. Man, Y. Chen, X. Jiang, L. Bian, L. Cui, B. Wei, G. Li, Synergistic effects on mesenchymal stem cell-based cartilage regeneration by chondrogenic preconditioning and mechanical stimulation. *Stem Cell Res. Ther.* **8**, 221 (2017).
45. Y. Rui, L. Xu, R. Chen, T. Zhang, S. Lin, Y. Hou, Y. Liu, F. Meng, Z. Liu, M. Ni, K. Sze Tsang, F. Yang, C. Wang, H. Chang Chan, X. Jiang, G. Li, Epigenetic memory gained by priming with osteogenic induction medium improves osteogenesis and other properties of mesenchymal stem cells. *Sci. Rep.* **5**, 11056 (2015).
46. L. Xu, Y. Liu, Y. Sun, B. Wang, Y. Xiong, W. Lin, Q. Wei, H. Wang, W. He, B. Wang, G. Li, Tissue source determines the differentiation potentials of mesenchymal stem cells: A comparative study of human mesenchymal stem cells from bone marrow and adipose tissue. *Stem Cell Res. Ther.* **8**, 275 (2017).
47. D. J. Craik, D. P. Fairlie, S. Liras, D. Price, The future of peptide-based drugs. *Chem. Biol. Drug Des.* **81**, 136–147 (2013).

Acknowledgments: We are grateful for the technical support from J. Lai, S. Wong, and A. Cheung from the School of Biomedical Sciences (The Chinese University of Hong Kong). We thank M. Zhu and K. Zhang for proofreading the manuscript. We sincerely thank M. Wong, N. So, K. Wei, M. Zhu, B. Yang, H. Chen, K. Zou, K. Zhang, Y. Jing, D. Siu Hong Wong, X. Xu, E. Yingrui Deng, X. Chen, and W. Li for the valuable discussions, support, and love. **Funding:** Project 31570979 is supported by the National Natural Science Foundation of China. The work described in this paper is supported by a General Research Fund grant from the Research Grants Council of Hong Kong (project nos. 14202215 and 14220716). This research is also supported by project BME-p3-15 of the Shun Hing Institute of Advanced Engineering (The Chinese University of Hong Kong). This work is supported by the Health and Medical Research Fund, the Food and Health Bureau, the Government of the Hong Kong Special Administrative Region (reference no. 04152836). This research is supported by the Chow Yuk Ho Technology Centre for Innovative Medicine (The Chinese University of Hong Kong). The work was partially supported by the Hong Kong Research Grants Council Theme-based Research Scheme (reference no. T13-402/17-N, Functional Bone Regeneration in Challenging Bone Disorders and Defects, 1 November 2017 to 31 October 2022). **Author contributions:** S.L. contributed to the animal experiments and analysis. M.Z. and J.X. contributed to the peptide synthesis and porous gel fabrication. Y.D. contributed to the cell culture and qPCR assay. X.C. contributed to the polymer synthesis and NMR characterization. K.W. contributed to the macromer synthesis and proofreading of the manuscript. R.L. contributed to the rest of the experiments and the manuscript. G.L. led the in vivo study of the project. L.B. led the project as the supervisor. **Competing interests:** The authors declare that they have no competing interests. **Data and materials availability:** All data needed to evaluate the conclusions in the paper are present in the paper and/or the Supplementary Materials. Additional data related to this paper may be requested from the authors.

Submitted 22 December 2018
Accepted 25 September 2019
Published 16 October 2019
10.1126/sciadv.aaw3896

Citation: R. Li, S. Lin, M. Zhu, Y. Deng, X. Chen, K. Wei, J. Xu, G. Li, L. Bian, Synthetic presentation of noncanonical Wnt5a motif promotes mechanosensing-dependent differentiation of stem cells and regeneration. *Sci. Adv.* **5**, eaaw3896 (2019).